An Experimental Study on the Entropy Generation during Fatigue of Fiber-Reinforced Thermoplastic Composites

Sara da Costa Pessoa
sarapessoa@tecnico.ulisboa.pt

Instituto Superior Técnico, Universidade de Lisboa, Portugal

July 2022

Abstract

Fracture fatigue entropy (FFE) is defined as the accumulated entropy at the time of fatigue failure, and several studies have proved it to be independent of the loading condition or stacking sequence, thus emerging as a promising fatigue failure criterion for metals and composites. However, the theoretical formulations for FFE in existing works are limited to materials with rate-independent behavior and to the best of the authors' knowledge, the concept of FFE has not yet been extended to thermoplastic composites neither theorically nor experimentally. The present work delivers a study on the effects of stress and frequency in the accumulated generated entropy due to plastic deformation and heat flux by conduction during fatigue using the Clausius-Duhem inequality. Fatigue tests were conducted on carbon fiber/PEKK dog-bone specimens with angle-ply and quasi-isotropic configurations at four test conditions comprising two stress levels and two loading frequencies. Full-field temperature measurements were obtained using an infrared thermal camera, while full-field in-plane strains were measured with a "low-cost" digital image correlation system. It was verified that FFE is not constant across all loading conditions for thermoplastic composites, which presented an accentuated rate-dependent behavior. The usefulness of FFE as a failure criterion might be compromised, highlighting the need to consider the influence of other dissipative terms on the total accumulated entropy.
Keywords: Thermoplastic Composites, Fatigue Life Prediction, Entropy Generation, Digital Image Correlation.

1. Introduction

For the past decades, the aerospace industry has been employing almost exclusively composites with thermoset matrices due to the well-established knowledge and certified processes available. Nevertheless, the incorporation of thermoplastic composites is becoming more common as they present advantages such as high impact toughness, higher damage tolerance, low moisture absorption, unlimited shelf life at ambient temperature, faster production cycles, and the ability to be recycled [1].

Since fatigue is one of the most critical phenomena affecting the structural integrity of components in engineering, a proper understanding of fatigue behavior is of the utmost importance. However, predicting the fatigue life of composites is a difficult task due to their heterogeneity, anisotropy, and presence of multiple damage modes. Also, the rate-dependent behavior of polymer matrix composites makes them highly susceptible to the loading frequency, which can result in a premature degradation of the material properties [2]. Several approaches for fatigue life prediction have been proposed, namely stress-life and energy-based methods. Yet, these methods are sensitive to the loading conditions and show a large scatter of data. The efforts to have a more unified fatigue failure criterion culminated in entropy-based approaches, as proposed by Naderi et al. [3]. The premise of their work is that fatigue damage accumulation is accompanied by irreversible energy dissipation, and such process generates entropy in accordance with the second law of thermodynamics. The concept of fracture fatigue entropy (FFE) is introduced as the cumulative entropy production up to the fracture point, and experimental studies proved it to be independent of loading amplitude, frequency, and geometry [4, 5, 6]. Most studies have been performed on metallic materials and a few on thermoset-based composites, but to the best of the authors' knowledge, this concept has not been applied to thermoplastics, whose effects of viscosity, temperature, and damage must be simultaneously considered. Moreover, entropy calculations performed in most studies disregarded the contribution of some dissipative terms under the assumption of having negligible or-

ders of magnitude for such materials. In this work, a similar approach to FFE is taken by calculating the dissipative terms already considered in previous works for tests at different loads, frequencies, and stacking sequences. On the other hand, a more comprehensive theoretical formulation is derived for further improvement of the generated entropy measurements.

2. Background

2.1. Thermodynamic laws

In the more general case of large deformations (or finite strains), body motion can be described from different standpoints depending on the configuration where position and time are being framed. Given that the initial geometry of the material is well known, all physical measures present in the following thermodynamic and constitutive laws will be represented with respect to an undeformed configuration. Using the localization theorem and a multiplicative decomposition of the deformation gradient, F, the balance of thermal energy can be expressed in the undeformed configuration as,

$$\rho_0 \dot{u} = \mathbf{S} \cdot \dot{\mathbf{E}} + \rho_0 r - \mathrm{Div} q_0, \tag{1}$$

where ρ_0 is the density in the undamaged configuration, u is the internal energy per unit mass, S is the second Piola-Kirchoff stress tensor, r is the generated energy per unit, $\dot{E}$ is the Lagrangian strain rate tensor, and q_0 is the heat flux transferred by conduction, convection, and radiation.

Based on the Clausius statement, the local form of the second law of thermodynamics can be written as,

$$\dot{\gamma}\theta = \mathbf{S} \cdot \dot{\mathbf{E}} - \rho_0 \left(\dot{\psi} + \theta \dot{\eta} \right) - q_0 \cdot \frac{\mathrm{Grad}\theta}{\theta} \geq 0, \tag{2}$$

where η and γ represent entropy per unit mass and unit volume, respectively, ψ is the Helmholtz free energy per unit mass, q_0 is the heat flux, and θ is the absolute temperature. In this work, the entropy of interest is γ that will be non-zero under the presence of dissipative phenomena. The respective representation for infinitesimal deformations yields,

$$\sigma \cdot \dot{\varepsilon} - \rho \left(\dot{\psi} + \dot{\theta} \eta \right) - \mathbf{q} \cdot \frac{\nabla \theta}{\theta} \geq 0. \tag{3}$$

The thermodynamic law of equation 3 imposes a natural condition to the mathematical description of the material's constitutive law.

2.2. Constitutive law and entropy generation

The Helmholtz free energy of the thermoplastic composite under study is assumed to be split into viscoelastic and viscoplastic components, $\psi(t) = \psi_{\mathrm{ve}}(t) + \psi_{\mathrm{vp}}(t)$. According to the thermodynamic theory for materials with memory, each component must be a function of the current and past histories of the variables in their respective arguments. Therefore, ψ_{ve} is assumed to be a functional of the viscoelastic infinitesimal strain ($\varepsilon_{\mathrm{ve}}$), the absolute temperature θ, and a scalar damage variable, D,

$$\psi_{\mathrm{ve}}(t) = \overset{\infty}{\underset{s=0}{\psi}} \left\{ \varepsilon_{\mathrm{ve}}(t-s), \theta(t-s), D(t-s) \right\}. \tag{4}$$

The viscoplastic component of the Helmholtz free energy is assumed to depend on the history of θ, and a kinematic hardening scalar variable, α,

$$\psi_{\mathrm{vp}}(t) = \overset{\infty}{\underset{s=0}{\psi}} \left\{ \theta(t-s), \alpha(t-s) \right\}. \tag{5}$$

The final form of the dissipation inequality can be obtained from integrating the following terms until the time of failure,

$$\theta\gamma = \int_0^{t_f} \sigma \cdot \dot{\varepsilon}_{\mathrm{vp}} - \mathbf{q} \cdot \frac{\nabla \theta}{\theta} - \rho \left(\dot{\eta}_v + \frac{\partial \psi_{\mathrm{vp}}}{\partial \alpha} \cdot \dot{\alpha}(t) + \frac{\partial \psi_{\mathrm{ve}}}{\partial D} \cdot \dot{D}(t) \right) dt \geq 0, \tag{6}$$

where η_v is the entropy per unit mass generated due to viscous phenomena. In the present work, focus will be given to the calculation of the first two terms of equation 6.

3. Implementation

3.1. Material processing

The composite used in this study is a carbon fiber reinforced polyetherketoneketone (PEKK). Prepreg tapes of Toray TC1320 were laid up into sixteen-ply plates using automated fiber placement and subjected to post-consolidation in the autoclave. Two stacking sequences were considered: angle-ply (AP) $[+45/\text{-}45]_{4s}$ and quasi-isotropic (QI) $[0/+45/\text{-}45/90]_{2s}$. The selection of these two stacking sequences is justified by the research interest underlying the temperature- and rate-dependent behavior of the thermoplastic matrix in the AP configuration and the high applicability of the QI configuration in aircraft components.

Specimens were cut from the plates using water-jet machining. Regarding the geometry of the specimens, it has been reported that the rectangular shape proposed by the ASTM D3479/D3479M standard test method for tension-tension fatigue of PMCs might not be adequate for high frequencies, failing within the gripping area [7]. To overcome this issue, the dog-bone geometry shown in Figure 1 was considered.

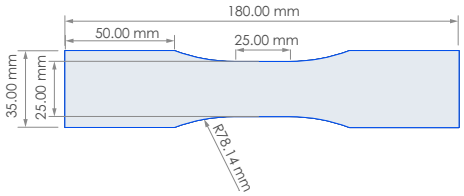

Figure 1: Specimen for fatigue testing.

3.2. Material characterization

Tensile tests to determine the material's ultimate tensile strength (UTS) were conducted at room temperature and strain rates as per the ASTM D3039. The properties at failure for each stacking sequence are shown in Table 1.

Table 1: Static tensile properties of the specimens.

	Maximum Load (kN)	Ultimate Strength (MPa)	Failure Strain(%)
AP	25.33	428.98	22.91
QI	37.90	630.75	1.30

Other important thermal-mechanical properties such as the composite's thermal conductivity along the loading direction, k_x, and speckle pattern's emissivity, e_{SP}, were measured and are summarized in Table 2.

Table 2: Thermal properties of the specimens.

	e_{SP}	k_x		
		25°C	50°C	100°C
AP	0.83	1.6482	1.6871	1.6885
QI		1.7497	1.8131	-

3.3. Experimental procedure

Fatigue tests in load-control mode with a load ratio R=0.1 were conducted using an Instron 8803 servo-hydraulic machine. To study the effect of frequency and stress level on the entropy generation, each stacking sequence was tested at four loading conditions by combining two frequencies (2Hz and 10Hz) and two maximum stress levels (70% and 80% of the UTS for the AP, and 85% and 95% for the QI).

The full-field surface temperature was captured using an infrared camera FLIR X6580sc, whereas the full-field strain field was measured with digital image correlation (DIC). However, traditional DIC cameras available were not able to capture strain data at the highest frequency, prompting the development of a new system. A digital single-lens reflex (DSLR) camera was chosen to record the fatigue test due to the high video recording frame rate and its low cost when compared to scientific-graded cameras. The parameters related to hardware and strain computation with DIC are stated in Table 3. A schematic of the developed procedure is illustrated in Figure 3. The experimental setup used for the fatigue tests comprising the aforementioned equipment is shown in Figure 2.

Table 3: DIC parameters.

Camera type	Nikon D3400
Lens	Nikkor 50mm f/1.8
Image size (px×px)	1920 × 1080
Video frame rate (Hz)	59.94
Aperture	1.8
Shutter speed	1/500
ISO	800
DIC software	GOM Correlate Pro
Facet size (px)	22
Point distance (px)	19

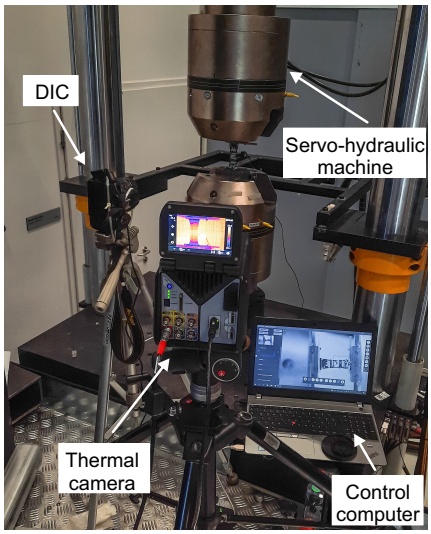

Figure 2: Experimental setup for fatigue testing.

4. Results

4.1. Angle-ply

4.1.1. Fatigue Behavior

The cyclic stress-strain behavior in fatigue is represented by the hysteresis loops. They consist of loading and unloading paths for each cycle, which do not overlap when viscoelasticity and plasticity occur. This deviation from ideal linear elasticity leads to energy losses in the material (hysteresis) that can be quantified by the area enclosed within the loops. The hysteresis curves for the four loading conditions are shown in Figure 4(a)-(d).

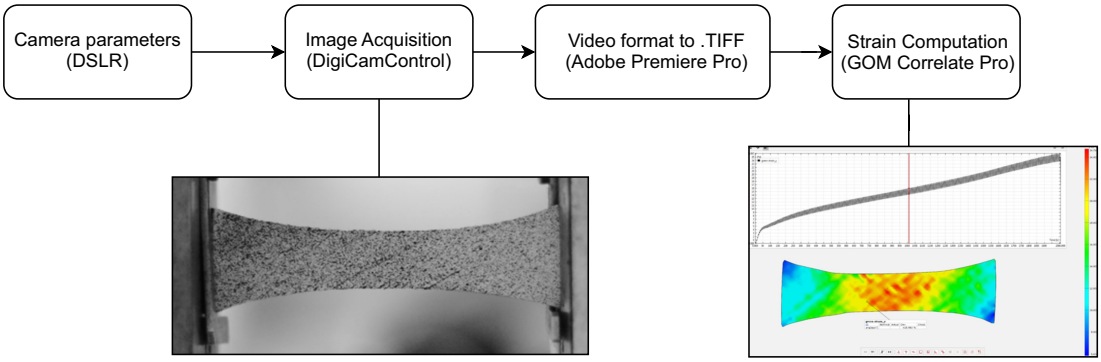

Figure 3: Experimental procedure for the developed "low-cost" DIC.

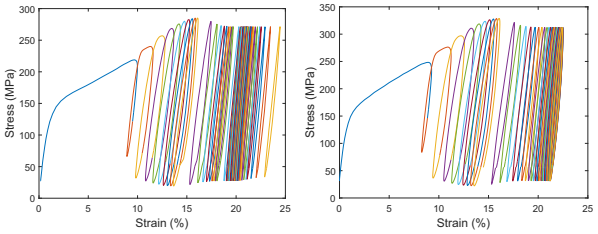

(a) AP 70% 2Hz (b) AP 80% 2Hz

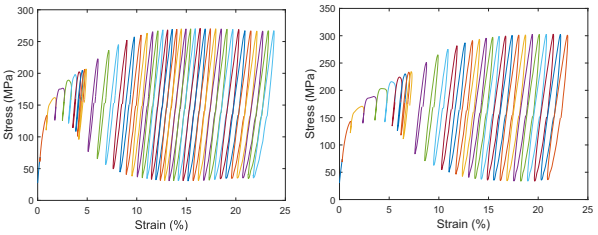

(c) AP 70% 10Hz (d) AP 80% 10Hz

Figure 4: Hysteresis loops of the AP specimens.

It is noticeable that tests run at the same frequency yield a similar overall evolution of the loops' area, and differ from the ones at another frequency, with higher dissipated energy in the early stages of the fatigue life for the lower frequency test cases. This observation is justified by the rate-dependent behavior of the PEKK since there is more time for the material to undergo greater deformations under the same applied stress level. For the higher frequency case, the strain response to the applied stress is more instantaneous, which resembles that of an elastoplastic material. In addition, most permanent deformation occurs in the first ten cycles of each test as evidenced by the difference in strain between the start and end points of the loops. During this period, as the maximum applied stress gradually approaches the target value, the yield point is still increasing due to the work hardening of the polymer, thus leading to significant plastic deformation. In every test case, shifting of the loops along the strain axis occurs. Such is characteristic of a fatigue-creep interaction caused by the non-zero mean stress and the rate-dependent behavior of the material. For tests at 2Hz, there is a decreasing cyclic-creep rate as seen by the loops overlapping after a number of cycles, translating into a stabilization in plastic strain accumulation, while 10Hz tests exhibit a continuous loop shift until failure.

4.1.2. Hysteresis Entropy

Following the entropy calculation approach of most of the related literature, the plastic work term in the RHS of equation (6) is assumed equal to the hysteresis energy. The evolution of the respective hysteresis-induced entropy and temperature with the normalized life of the material is plotted in Figure 5.

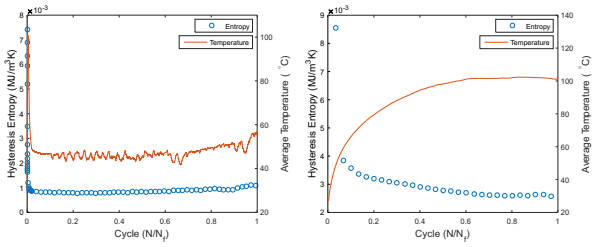

(a) AP 70% 2Hz (b) AP 80% 2Hz

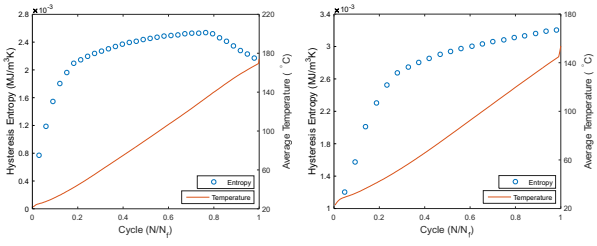

(c) AP 70% 10Hz (d) AP 80% 10Hz

Figure 5: Hysteresis entropy and temperature evolution in AP specimens.

Similar trends of entropy evolution can be observed for tests conducted at the same loading frequency, in accordance with the findings reported in Section 4.1.1. An increase in entropy generation followed by a linear rise in average temperature to

near the glass transition temperature ($T_g = 160°C$) for the 10Hz cases can be observed in Figures 5(c) and (d). The high loading frequency combined with the low thermal conductivity of the matrix material prevents energy due to irreversible phenomena from dissipating to the environment, thus leading to adiabatic heating. The subsequent increase in temperature is stored in the system as internal energy that can be measured in the hysteresis loops as per equation 1. On the other hand, the entropy generated in each cycle at 2Hz follows a decreasing trend over the fatigue life accompanied by a temperature profile that stabilizes below the glass transition temperature. The lower loading rate allows for the PEKK to undergo larger strains as depicted in Figures 5(a) and (b), hence contributing to a high initial plastic work-induced dissipation. Due to work hardening, the energy generated due to mechanical dissipative phenomena decreases during the material's lifetime which coupled with the low loading frequency allows for the material to exchange energy with the environment. At this stage, thermal equilibrium is attained, and the temperature remains fairly constant until failure.

4.1.3. Thermal Dissipation Entropy

During the fatigue test, heat flows from the specimen to the machine grips by conduction. Using Fourier's law to quantify q_k in equation (6), the evolution of entropy flow due to the heat flux for the AP 70% 10Hz case is shown in Figure 6. This term can be assumed negligible since its order of magnitude (10^{-5}) is lower than the one of the hysteresis entropy (10^{-3}). The case chosen for this analysis is the one presenting higher temperatures, thus thermal dissipation entropy can be confidently assumed to be negligible for the remaining cases with similar or lower temperatures, as less heat is dissipated by conduction. For this reason, the results obtained in the previous section remain unchanged, proving that hysteresis prevails over heat conduction for a composite under large temperature gradients.

4.1.4. Accumulated Entropy

Finally, the accumulation of entropy throughout the test was determined by cumulatively summing the generated entropy per cycle. The values of γ at failure (i.e., FFE in MJ/m^{3}K) and fatigue life (N_f) for each loading case are presented in Table 4.

Table 4: FFE and fatigue life of AP specimens.

		2Hz		**10Hz**	
70%	FFE	52.52	58.98	0.7323	0.7414
	N_f	50 332	56 784	327	334
80%	FFE	0.9976	1.0421	0.6026	0.6224
	N_f	299	350	214	221

Unlike most conclusions drawn in related literature, the accumulated entropy at failure due to plastic work for the thermoplastic composite under study is not constant. When the fatigue life increases by over 150 times in the AP 70% 2Hz case, FFE also increases, although non-proportionally. The reason is there are more cycles adding up to the final value, whereas the order of magnitude of the entropy generated per cycle is not sufficiently lower to yield a constant FFE. However, it can also be inferred from the AP 80% 2Hz and AP 70% 10Hz cases that more cycles do not always yield a higher FFE. Figure 7 shows the accumulated entropy vs. cycles for one test of each loading condition, where different rates of entropy accumulation can be seen. Different rates are a necessary condition to have a similar value at failure for different fatigue lives, which may derive from different stress- and strain-rates imposed by the loading frequency and stress level or phenomena associated with damage. For this material, however, the rates are not different enough to yield such results, thus an approach that includes or excludes the contribution of other terms is required.

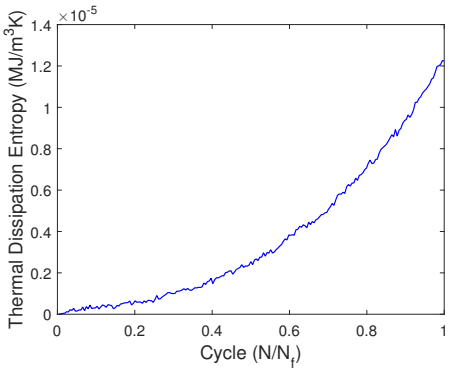

Figure 6: Entropy generated due to heat transfer for the AP 70% 10Hz case.

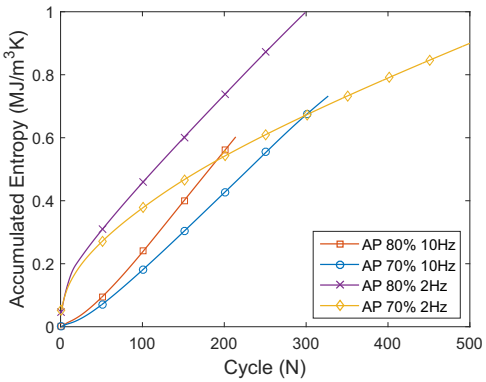

Figure 7: Accumulated entropy through the cycles in AP specimens.

In addition, the normalized accumulated entropy is also not linearly correlated with the normalized fatigue life and every test case follows a different trend, as seen in Figure 8. This means the equation for the failure criterion proposed in the literature, $\frac{N}{N_f} = \frac{\gamma}{FFE}$, is not applicable, thus compromising the usefulness of entropy as fatigue life prediction method for thermoplastic composites.

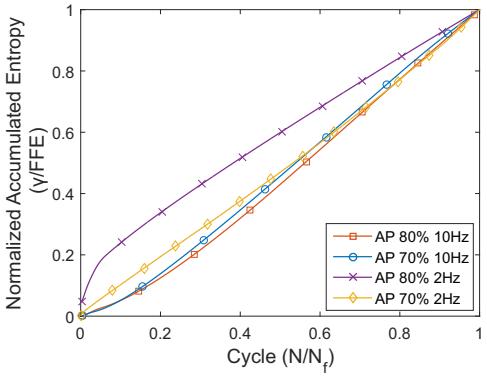

Figure 8: Accumulated entropy throughout the life of AP specimens.

4.1.5. Infinitesimal vs. Finite Strain Assumptions

The AP specimens develop strains of up to 25% at the time of failure, which is considered to be in the realm of large deformations. The entropy was recalculated using the formulation derived with finite strain theory in equation 2 and the new values of FFE alongside the ones obtained with infinitinesal strains are presented in Table 5. The FFE values of the loading conditions that yield a short fatigue life are not greatly affected by the infinitesimal approximation, contrary to the test that lasted 50 000 cycles. Regardless, this source of error does not have an impact on the conclusions drawn about the nonconstancy of FFE. Yet, the accuracy is affected and finite strain theory should be considered for future work on this stacking sequence.

Table 5: FFE (MJ/m^{3}K) calculated with infinitesimal vs finite strain theory.

		2Hz		**10Hz**	
		$\sigma \cdot \dot{\varepsilon}$	$\mathbf{S} \cdot \dot{\mathbf{E}}$	$\sigma \cdot \dot{\varepsilon}$	$\mathbf{S} \cdot \dot{\mathbf{E}}$
70%	FFE	52.52	44.12	0.7323	0.7321
	N_f	50 332		327	
80%	FFE	0.9976	1.001	0.6026	0.6023
	N_f	299		214	

4.2. Quasi-isotropic

4.2.1. Fatigue Behavior

For the QI specimens, a similar analysis as in Section 4.1 was performed. The hysteresis curves for all the testing conditions are shown in Figure 9.

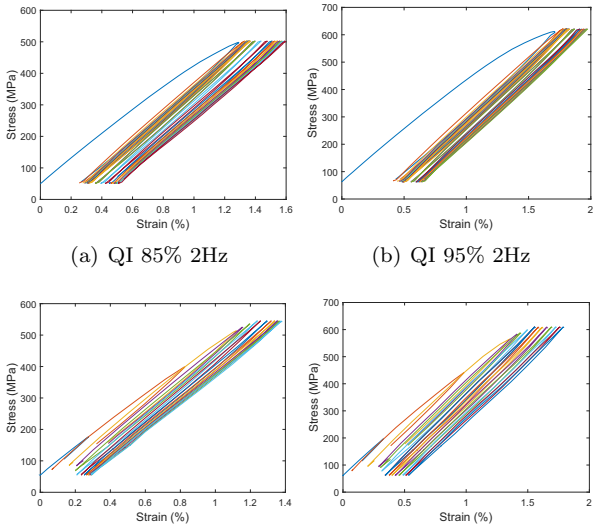

(a) QI 85% 2Hz (b) QI 95% 2Hz

(c) QI 85% 10Hz (d) QI 95% 10Hz

Figure 9: Hysteresis loops of the QI specimens.

The hysteresis loops are almost overlapping with a small shift in strain throughout the entire test, showing that nonsignificant irreversible deformation occurs. Also, the areas inside the hysteresis loops are smaller than the ones of the AP laminate, which indicates that most dissipation is originated in the matrix, and it is not as pronounced when fibers are being loaded axially. Moreover, the higher magnitude of plastic deformation accumulated during the first loading cycles and total strain for the 2Hz cases reveal the rate-dependent behavior of the laminate introduced by some of the off-axis plies in uniaxial loading.

4.2.2. Hysteresis Entropy

Figure 9 represents the evolution of entropy generated per cycle throughout the normalized fatigue life for each of the loading cases. A decreasing trend independent of loading frequency and stress level with a steeper decay within the first 10% of the life can be observed. This initial evolution agrees well with trends of stiffness and temperature evolution in polymer composites where matrix cracking is expected to be more pronounced. Furthemore, more entropy is being generated per cycle for the higher load at the same frequency level, and for the higher frequency at the same load level. It is also observed that QI specimens generate less entropy than their AP counterparts, which underlines the prevailing role of the matrix in dissipative phenomena.

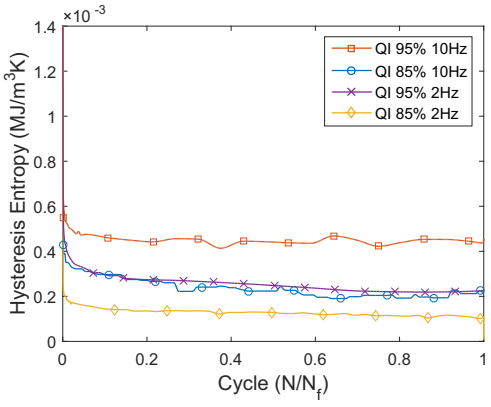

Figure 10: Entropy generated due to hysteresis in QI specimens.

4.2.3. Thermal Dissipation Entropy

Since the hysteresis entropy in QI specimens is one order of magnitude below the one of the AP laminate, the assumption of negligible entropy due to heat transfer must be confirmed. Figure 11 presents the evolution of the thermal dissipation entropy with cycles. It can be concluded that this form of entropy generation remains negligible for this configuration.

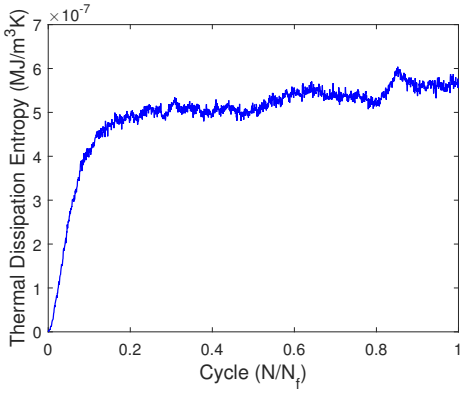

Figure 11: Entropy generated due to heat transfer for the QI 95% 10Hz case.

4.2.4. Accumulated entropy

The values of FFE (in MJ/m^{3}K) and fatigue life (N_f) for each loading case are presented in Table 6. Similar to the conclusions drawn for the AP case in section 4.1.4, the accumulated entropy at failure is not constant also for a fiber-dominated configuration. In addition, FFE does not vary linearly with the number of cycles to failure, since tests with a higher fatigue life can present lower FFE (case QI 85% 2Hz vs QI 95% 10Hz]). In order to have a better understanding about the root of non-constant FFE, the accummulated entropy along the cycles is plotted in Figure 12. A set of features that have never been mentioned in the related literature can

Table 6: FFE and fatigue life of QI specimens.

		2Hz		10Hz	
85%	FFE	5.172	6.905	20.87	22.85
	N_f	40 352	53 871	77 479	91 813
95%	FFE	0.5504	1.783	8.382	8.759
	N_f	2 285	6 969	18 564	19 614

be analysed. Firstly, each loading condition yields a different rate of entropy accumulation, where an increase in load and frequency resulting in a higher rate. However, such difference in rates is still not enough to match FFE for different fatigue lives. On the other hand, for tests perfomed on different specimens at the same strain-rate (same loading amplitude and frequency), entropy accumulates at the same rate although they present different fatigue lives. For this reason, it proves that computing entropy and FFE from the hysteresis energy is not a suitable approach for this material, since it does not capture any information about the imminence of failure.

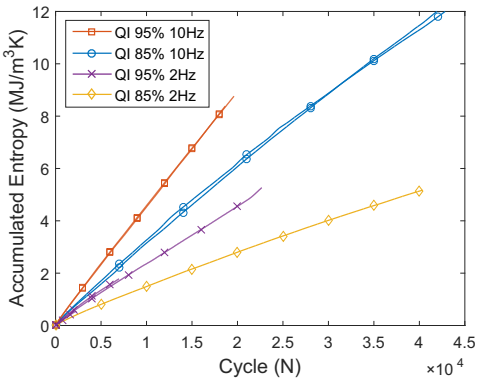

Figure 12: Accumulated entropy through the cycles in QI specimens.

Regarding the relationship between the normalized accumulated entropy and normalized cycles, Figure 13 shows that its non-linearity is not as accentuated as in the AP specimens. Only the QI 95% 10Hz case presents a perfectly linear correlation, while for the remaining cases, the trend is similar among them, though not exactly linear. If a constant FFE is achievable in future work and a similar trend is still verified, a modification to the failure criteria should be made. A suggestion is assuming a power-law correlation as $\left(\frac{N}{N_f}\right)^n = \frac{\gamma}{FFE}$.

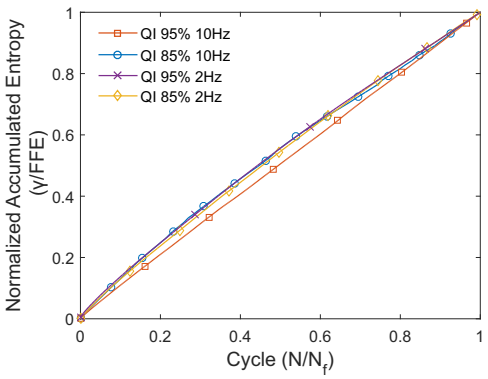

Figure 13: Accumulated entropy throughout the life of QI specimens.

4.3. Entropy as a failure criterion

As it was verified in the previous sections, the entropy calculation approach based on the hysteresis energy and thermal dissipation (although negligible) is insufficient to prove the usefulness of entropy as a failure criterion. The FFE results of all tests performed are plotted against the fatigue life in Figure 14 and no constant value can be assumed to exist.

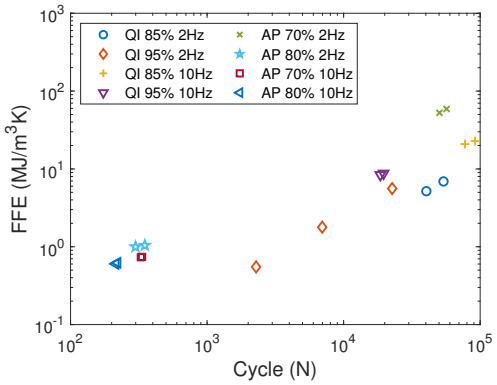

Figure 14: FFE vs. fatigue life.

While the approach used in the present work to calculate entropy is identical to the ones in the related literature, the drawn conclusions about FFE are not replicated. The root of such difference with the previous studies on epoxy-based composites can be attributed to the higher sensitivity of thermoplastics to the loading conditions, reflected on the disparate values of fatigue life and entropy generation between different test cases.

Another factor contributing to the lack of a unified FFE value is the presence of energy generated due to non-damaging terms, such as internal friction (IF), in the hysteresis area. Recent works demonstrated that constant FFE can only be achieved if the effects of IF are removed [8, 9]. However, the methods for quantification of internal friction used in those studies are not applicable beyond the realm of linear elasticity, which disregards IF phenomena due to the non-linear and viscous behavior observed in thermoplastics. Nonetheless, the approach used in [8] was attempted for the QI laminate, as this configuration presents a static mechanical behavior comparable to that of a linear elastic material. Figure 15 compares the accumulated entropy for QI specimens before and after removing internal friction. It can be observed that the effect of this removal is solely reflected in a proportional reduction of the entropy accumulation rate in all cases. A well-marked dependence on loading conditions is still verified, not affecting the trend of FFE results.

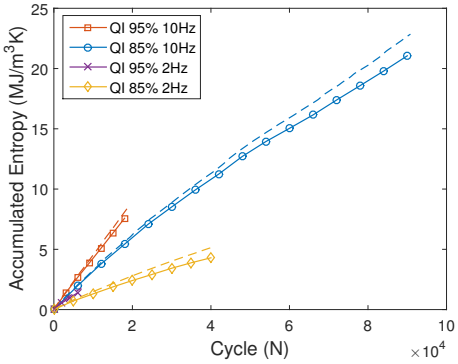

Figure 15: Accumulated entropy through the cycles in QI specimens with (dashed line) and without IF (solid line).

Since the determination of energy related to IF is a difficult task, an alternative to quantify the mechanical work term due to irreversible deformations is proposing a cyclic plasticity model instead of using the area within the hysteresis loops.

The non inclusion of other dissipative terms in the entropy balance may also constitute a source of error. As an example, the energy related to damage is expected to be 30-50% of the energy generation in composite materials [10]. For that reason, the implementation of a damage parameter that accurately reflects the damage evolution in the material during fatigue is of the utmost importance. The concept of fatigue modulus [11] can be used to describe isotropic damage in the specimen and relies on data collected during each fatigue test, which greatly simplifies its implementation. Damage can be parametrized as a scalar variable, D, as follows,

$$D(N) = 1 - \frac{F(N)}{F_0}, \tag{7}$$

where F_0 and $F_(N)$ are the fatigue modulus in the first loading and at cycle N, respectively. An inverse power law was verified for tests across all loading conditions, as shown for a representative case of

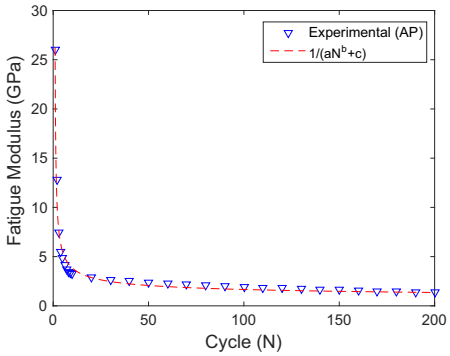

(a) AP specimens

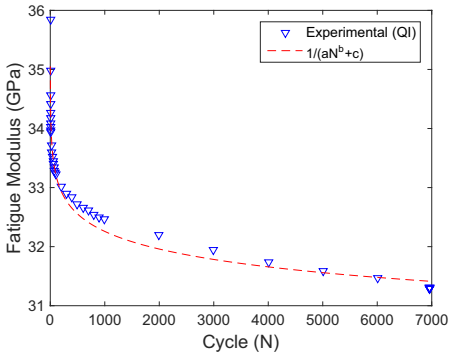

(b) QI specimens

Figure 16: Fatigue modulus evolution with the number of cycles.

each stacking sequence in Figure 16. In addition, phenomena related to hardening and viscosity can influence the FFE values as well, and should be considered for the accuracy of results.

5. Conclusions

The entropy generated due to dissipative phenomena during fatigue of PEKK-carbon fiber reinforced composites subjected to different stress and frequency levels was experimentally measured using the hysteresis energy. Contrary to findings reported in the literature, the entropy generated at the time of failure is not constant across all loading conditions and stacking sequences which precludes the implementation of entropy as a failure criterion for thermoplastic composites.

Future work following this thesis can focus on accounting for viscous, damage, and hardening phenomena in the total generated entropy, using the proposed constitutive law as a starting point.

Acknowledgements

The financial and infrastructural support provided by Sabanci University - Integrated Manufacturing Technologies Research and Application Center, Sabanci University - Kordsa Composite Technologies Center of Excellence, and the individual research grant are greatly appreciated.

References

[1] P.E. Irving and C. Soutis(Eds.). *Polymer composites in the aerospace industry*. Woodhead Publishing, 2nd edition, 2020. ISBN 978-0-08-102679-3.

[2] (Ed.) B. Harris. *Fatigue in composites: science and technology of the fatigue response of fibre-reinforced plastics*. Woodhead Publishing, 2003. ISBN 0-203-48371-5.

[3] M. Naderi, M. Amiri, and M.M. Khonsari. On the thermodynamic entropy of fatigue fracture. *Proceedings of the Royal Society A: Mathematical, Physical and Engineering Sciences*, 466(2114):423–438, 2010.

[4] M. Naderi and M.M. Khonsari. Thermodynamic analysis of fatigue failure in a composite laminate. *Mechanics of Materials*, 46:113–122, 2012.

[5] B. Mohammadi and A. Mahmoudi. Developing a new model to predict the fatigue life of cross-ply laminates using coupled CDM-entropy generation approach. *Theoretical and Applied Fracture Mechanics*, 95:18–27, 2018.

[6] J. Huang, C. Li, and W. Liu. Investigation of internal friction and fracture fatigue entropy of CFRP laminates with various stacking sequences subjected to fatigue loading. *Thin-Walled Structures*, 155:106978, 2020.

[7] D.C. Curtis, D.R. Moore, B. Slater, and N. Zahlan. Fatigue testing of multi-angle laminates of CF/PEEK. *Composites Evaluation*, pages 40–50, 1987. Butterworth-Heinemann.

[8] M. Liakat and M.M. Khonsari. On the anelasticity and fatigue fracture entropy in high-cycle metal fatigue. *Materials & Design*, 82:18–27, 2015.

[9] J.Y. Jang and M.M. Khonsari. On the evaluation of fracture fatigue entropy. *Theoretical and Applied Fracture Mechanics*, 96:351–361, 2018.

[10] E. K. Gamstedt, O. Redon, and P. Brøndsted. Fatigue dissipation and failure in unidirectional and angle-ply glass fibre/carbon fibre hybrid laminates. *Key Engineering Materials*, 221:35–48, 2002. Trans Tech Publications Ltd.

[11] W. Hwang and K. S. Han. Fatigue of composites — fatigue modulus concept and life prediction. *Journal of Composite Materials*, 20(2):154–165, 1986.